energetically optimized by using several cycles of molecular dynamics calculations with X-PLOR[28] and two-fold symmetry restraints between the two subunits in the dimer.

Received 5 March; accepted 21 June 1999.

1. Falke, J. J., Bass, R. B., Butler, S. L., Chervitz, S. A. & Danielson, M. A. The two-component signaling pathway of bacterial chemotaxis: a molecular view of signal transduction by receptors, kinases, and adaptation enzymes. *Annu. Rev. Cell Biol. Dev. Biol.* **13,** 457–512 (1997).
2. Ullrich, A. & Schlessinger, J. Signal transduction by receptors with tyrosine kinase activity. *Cell* **61,** 203–212 (1990).
3. Chervitz, S. A. & Falke, J. J. Molecular mechanism of transmembrane signaling by the aspartate receptor: a model. *Proc. Natl Acad. Sci. USA* **93,** 2545–2550 (1996).
4. Le Moual, H. & Koshland, D. E. Jr Molecular evolution of the C-terminal cytoplasmic domain of a superfamily of bacterial receptors involved in taxis. *J. Mol. Biol.* **261,** 568–585 (1996).
5. Cochran, A. G. & Kim, P. S. Imitation of *Escherichia coli* aspartate receptor signaling in engineered dimers of the cytoplasmic domain. *Science* **271,** 1113–1116 (1996).
6. Ames, P., Yu, Y. A. & Parkinson, J. S. Methylation segments are not required for chemotactic signalling by cytoplasmic fragments of Tsr, the methyl-accepting serine chemoreceptor of *Escherichia coli*. *Mol. Microbiol.* **19,** 737–746 (1996).
7. Surette, M. G. & Stock, J. B. Role of α-helical coiled-coil interactions in receptor dimerization, signaling, and adaptation during bacterial chemotaxis. *J. Biol. Chem.* **271,** 17966–17973 (1996).
8. Maddock, J. R. & Shapiro, L. Polar location of the chemoreceptor complex in the *Escherichia coli* cell. *Science* **259,** 1717–1723 (1993).
9. Liu, Y., Levit, M., Lurz, R., Surette, M. G. & Stock, J. B. Receptor-mediated protein kinase activation and the mechanism of transmembrane signaling in bacterial chemotaxis. *EMBO J.* **16,** 7231–7240 (1997).
10. Chi, Y. I., Yokota, H. & Kim, S.-H. Apo structure of the ligand-binding domain of aspartate receptor from *Escherichia coli* and its comparison with ligand-bound or pseudoligand-bound structures. *FEBS Lett.* **414,** 327–332 (1997).
11. Lynch, B. A. & Koshland, D. E. Jr The fifth Datta Lecture. Structural similarities between the aspartate receptor of bacterial chemotaxis and the trp repressor of *E. coli*. Implications for transmembrane signaling. *FEBS Lett.* **307,** 3–9 (1992).
12. Gardina, P. J. & Manson, M. D. Attractant signaling by an aspartate chemoreceptor dimer with a single cytoplasmic domain. *Science* **274,** 425–426 (1996).
13. Tatsuno, I., Homma, M., Oosawa, K. & Kawagishi, I. Signaling by the *Escherichia coli* aspartate chemoreceptor Tar with a single cytoplasmic domain per dimer. *Science* **274,** 423–425 (1996).
14. Hughson, A. G. & Hazelbauer, G. L. Detecting the conformational change of transmembrane signaling in a bacterial chemoreceptor by measuring effects on disulfide cross-linking *in vivo*. *Proc. Natl Acad. Sci. USA* **93,** 11546–11551 (1996).
15. Milburn, M. V. *et al.* Three-dimensional structures of the ligand-binding domain of the bacterial aspartate receptor with and without a ligand. *Science* **254,** 1342–1347 (1991).
16. Kim, S.-H. "Frozen" dynamic dimer model for transmembrane signaling in bacterial chemotaxis receptors. *Protein Sci.* **3,** 159–165 (1994).
17. Maruyama, I. N., Mikawa, Y. G. & Maruyama, H. I. A model for transmembrane signaling by the aspartate receptor based on random-cassette mutagenesis and site-directed disulfide cross-linking. *J. Mol. Biol.* **253,** 530–546 (1995).
18. Borkovich, K. A., Alex, L. A. & Simon, M. I. Attenuation of sensory receptor signaling by covalent modification. *Proc. Natl Acad. Sci. USA* **89,** 6756–6760 (1992).
19. Ames, P. & Parkinson, J. S. Transmembrane signaling by bacterial chemoreceptors: *E. coli* transducers with locked signal output. *Cell* **55,** 817–826 (1988).
20. Ames, P., Chen, J., Wolff, C. & Parkinson, J. S. Structure–function studies of bacterial chemosensors. *Cold Spring Harb. Symp. Quant. Biol.* **53,** 59–65 (1988).
21. Danielson, M. A., Bass, R. B. & Falke, J. J. Cysteine and disulfide scanning reveals a regulatory α-helix in the cytoplasmic domain of the aspartate receptor. *J. Biol. Chem.* **272,** 32878–32888 (1997).
22. Bass, R. B. & Falke, J. J. Detection of a conserved α-helix in the kinase docking region of the aspartate receptor by cysteine and disulfide scanning. *J. Biol. Chem.* **273,** 25006–25014 (1998).
23. Kunkel, T. A. Rapid and efficient site-specific mutagenesis without phenotypic selection. *Proc. Natl Acad. Sci. USA* **82,** 488 (1985).
24. Jancarik, J. & Kim, S.-H. Sparse matrix sampling: a screening method for crystallization of proteins. *J. Appl. Crystallogr.* **24,** 409–411 (1991).
25. Otwinowski, Z. in *Data Collection and Processing* (eds Sawyer, L., Isaacs, N. & Bailey, S.) 56–62 (SERC Daresbury Laboratory, Warrington, UK, 1993).
26. Collaborative Computing Project No. 4. The CCP4 suite: Programs for protein crystallography. *Acta Crystallogr. D* **50,** 760–763 (1994).
27. Jones, T. A., Zou, J.-Y., Cowan, S. W. & Kjeldgaard, M. Improved methods for binding protein models inelectron density maps and the location of errors in these models. *Acta Crystallogr. A* **47,** 110–119 (1991).
28. Brünger, A. T. *X-PLOR Version 3.1* (Yale Univ. Press, New Haven, CT, 1993).
29. Laskowski, R. A., MacArthur, M. W., Moss, D. S. & Thronton, J. M. Procheck: A program to check the stereochemical quality of protein structures. *J. Appl. Crystallogr.* **26,** 283–291 (1993).
30. Kraulis, P. I. MOLSCRIPT: a program to produce both detailed and schematic plots of protein structures. *J. Appl. Crystallogr.* **24,** 946–950 (1991).

Acknowledgements. We thank R. Sweet, P. Kuhn and H. Bellamy for data collection; D. King for performing the electrospray mass spectrometry; C. Park for plasmid HB915; K. Kamata for help with sample preparation; Z. Zhang and E. Berry for preparing some of the figures; and J. Falke and S. Parkinson for discussion. This work was supported by grants from the Office of Biological and Environmental Research, Office of Science, DOE and the NIH.

Correspondence and requests for materials should be addressed to S.H.K. at the Melvin Calvin Laboratory (e-mail: shkim@LBL.gov). The accession code for the atomic coordinates of the structure at the Protein Data Bank is 1QU7.

errata

p73 is regulated by tyrosine kinase c-Abl in the apoptotic response to DNA damage

Zhi-Min Yuan, Hisashi Shioya, Takatoshi Ishiko, Xiangao Sun, Jijie Gu, YinYin Huang, Hua Lu, Surender Kharbanda, Ralph Weichselbaum & Donald Kufe

Nature **399,** 814–817 (1999)

Figure 2e as published was a duplicate of Fig. 2d. The correct figure is shown below. □

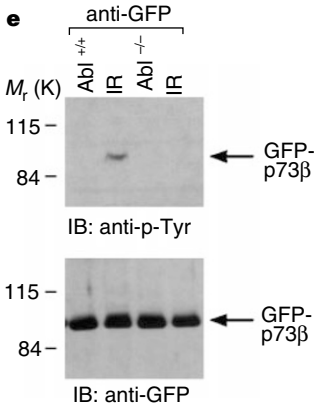

Regulation of endothelium-derived nitric oxide production by the protein kinase Akt

David Fulton, Jean-Philippe Gratton, Timothy J. McCabe, Jason Fontana, Yasushi Fujio, Kenneth Walsh, Thomas F. Franke, Andreas Papapetropoulos & William C. Sessa

Nature **399,** 597–601 (1999)

In Fig. 2c, the lower panel was incorrectly shifted to the right: the figure should have appeared as below. In Fig. 4b, the concentration of free calcium was in micromolar, and not millimolar as published. □

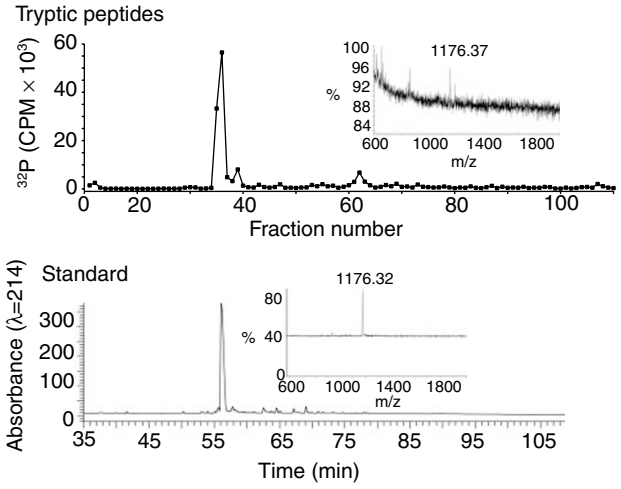

© 1999 Macmillan Magazines Ltd

p73 is regulated by tyrosine kinase c-Abl in the apoptotic response to DNA damage

Zhi-Min Yuan*†, Hisashi Shioya†, Takatoshi Ishiko†, Xiangao Sun†, Jijie Gu*†, YinYin Huang†, Hua Lu‡, Surender Kharbanda†, Ralph Weichselbaum§ & Donald Kufe*†

** Department of Cancer Cell Biology, Harvard School of Public Health,*
† Dana-Farber Cancer Institute, Harvard Medical School, 44 Binney Street, Boston, Massachusetts 02115, USA
‡ Department of Biochemistry and Molecular Biology, Oregon Health Science University, Portland, Oregon 97201, USA
§ Department of Radiation and Cellular Oncology, University of Chicago, Chicago, Illinois 60637, USA

The protein p73 is a structural and functional homologue of the p53 tumour-suppressor protein but, unlike p53, it is not induced in response to DNA damage[1,2]. The tyrosine kinase c-Abl is activated by certain DNA-damaging agents[3] and contributes to the induction of programmed cell death (apoptosis) by p53-dependent and p53-independent mechanisms[4]. Here we show that c-Abl binds to p73 in cells, interacting through its SH3 domain with the carboxy-terminal homo-oligomerization domain of p73. c-Abl phosphorylates p73 on a tyrosine residue at position 99 both *in vitro* and in cells that have been exposed to ionizing radiation. Our results show that c-Abl stimulates p73-mediated transactivation and apoptosis. This regulation of p73 by c-Abl in response to DNA damage is also demonstrated by a failure of ionizing-radiation-induced apoptosis after disruption of the c-Abl–p73 interaction. These findings show that p73 is regulated by a c-Abl-dependent mechanism and that p73 participates in the apoptotic response to DNA damage.

Because c-Abl mediates DNA-damage-induced apoptosis in a p53-independent way[4] and p73 contributes to the induction of apoptosis[1,2], we investigated whether c-Abl interacts with p73 by immunoblotting anti-c-Abl immunoprecipitates from COS7 cells with anti-p73. The results demonstrate constitutive binding of c-Abl and p73; as a control, there was no detectable p73 in anti-RPA70 immunoprecipitates (Fig. 1a). As c-Abl is activated by DNA damage[3,5–8], we tested whether c-Abl associates with p73 after exposure to ionizing radiation. Analysis of anti-c-Abl immunoprecipitates with anti-p73 indicated that c-Abl bound to p73 in both control and irradiated cells (Fig. 1b). We also prepared ^{35}S-labelled p73α and p73β by *in vitro* transcription/translation for incubation with Abl fusion proteins with glutathione-*S*-transferase (GST). Analysis of the adsorbates demonstrated binding between GST–Abl SH3 and the p73α isoform[1], but not with a GST fusion protein prepared from the c-Abl SH2 domain; results were similar with GST–Abl SH3 and p73β (Fig. 1c). p73 contains an amino-terminal acidic transactivation domain (TAD), a central DNA-binding core domain (DBD) and a C-terminal homo-oligomerization domain (OD)[1]. We incubated *in vitro* transcribed and translated proteins containing the different p73 domains with GST–Abl SH3. Analysis of these adsorbates demonstrated that the c-Abl SH3 domain binds to the OD, but not the TAD or DBD, of p73 (Fig. 1d). To confirm these findings, we assayed mutants of p73β deleted at amino acids 311–419 and 419–494 for binding to c-Abl SH3. The results demonstrate binding of c-Abl SH3 to p73β(Δ419–494) but not to p73β(Δ311–419) (not shown), indicating that c-Abl associates with the p73 C-terminal homo-oligomerization domain.

To determine whether c-Abl phosphorylates p73, we incubated recombinant c-Abl with immuno-purified Flag-tagged p73α and p73β in the presence of [^{32}P]ATP. Analysis of the products by autoradiography showed that both p73α and p73β are substrates for c-Abl *in vitro* (Fig. 2a, left), but there was no detectable phosphorylation of p73α or p73β when c-Abl was substituted with recombinant kinase-inactive c-Abl(K-R)[9] (data not shown). In addition, c-Abl-mediated phosphorylation of p73β was prevented in a p73β(Y-F) mutant in which Tyr 99 (YAQP) was altered to phenylalanine (FAQP) (Fig. 2a, right). As a control, mutation of Tyr 121 (YPGP) to phenylalanine had little if any effect on c-Abl-mediated phosphorylation (Fig. 2a, right). To test whether p73 is phosphorylated by c-Abl *in vivo*, we co-transfected 293 cells with c-Abl and GFP–p73β, in which p73β was tagged with green fluorescent protein (GFP). Analysis of anti-GFP immunoprecipitates with anti-phosphotyrosine antibody (anti-P-Tyr) demonstrated tyrosine phosphorylation of p73β (Fig. 2b, left). By contrast, co-transfection of the kinase-inactive c-Abl(K-R) mutant and GFP–p73β resulted in no apparent tyrosine phosphorylation of p73β (Fig. 2b, left). In addition, there was no detectable c-Abl-mediated phosphorylation of the p73β(Y^{99}-F) mutant (Fig. 2b, right). To assess whether p73 is phosphorylated in response to DNA damage, we irradiated COS7 cells which express high levels of endogenous p73α and p73β (ref. 10). Analysis of anti-p73 immunoprecipitates with anti-P-Tyr demonstrated tyrosine phosphorylation of p73 in irradiated, but not control, cells (Fig. 2c). To determine whether irradiation-induced tyrosine phosphorylation of p73 is c-Abl-dependent, we used MCF-7 cells which stably express the empty pSR vector or c-Abl(K-R)[11]; these cells were transfected to express

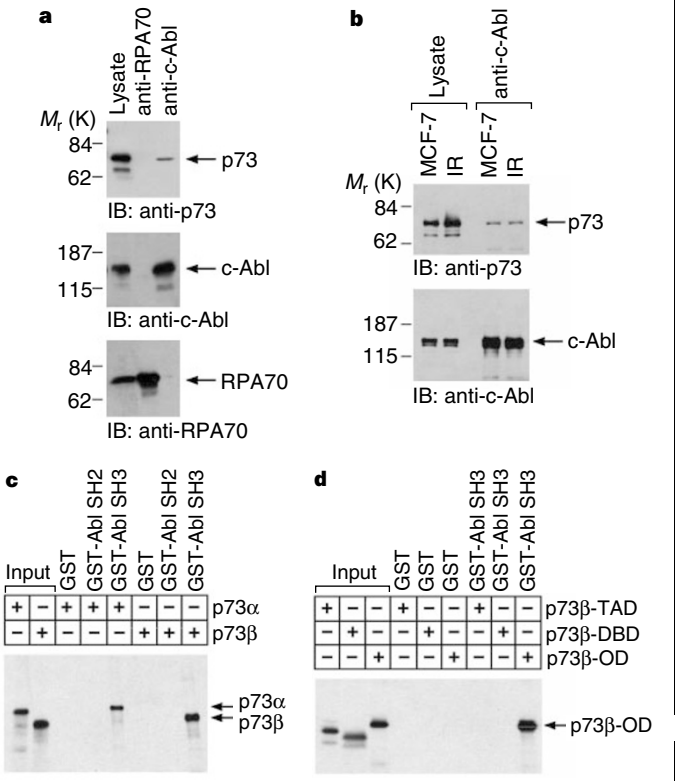

Figure 1 Association of c-Abl and p73. **a**, Lysates from COS7 cells were immunoprecipitated with anti-RPA70 or anti-c-Abl. The immunoprecipitates were analysed by immunoblotting (IB) with anti-p73, anti-c-Abl or anti-RPA70. Lysate was directly analysed by immunoblotting as a control. **b**, MCF-7 cells were exposed to 20 Gy of ionizing radiation (IR) and collected 1 h later. Lysates were analysed by immunoblotting with anti-p73 or anti-c-Abl (left two lanes), or immunoprecipitated with anti-c-Abl and the precipitates immunoblotted with anti-GFP, anti-p73 or anti-c-Abl (two right lanes). **c**, ^{35}S-labelled Flag–p73α and Flag–p73β were incubated with GST, GST–AblSH2 or GST–AblSH3 fusion proteins. Adsorbates were analysed by SDS–PAGE and autoradiography. **d**, ^{35}S-labelled Flag–p73β TAD, Flag–p73β DBD and Flag–p73β OD were incubated with GST or GST–AblSH3. Adsorbates were analysed as in **c**.

© 1999 Macmillan Magazines Ltd

GFP–p73β and then exposed to 20 Gy ionizing radiation. Lysates were immunoprecipitated with anti-GFP and the precipitates were immunoblotted with anti-P-Tyr. The results demonstrate tyrosine phosphorylation of p73β in irradiated, but not control, MCF-7/pSR cells (Fig. 2d). By contrast, there was no detectable tyrosine phosphorylation of p73β in irradiated MCF-7/c-Abl(K-R) cells (Fig. 2d). To confirm that p73 is phosphorylated by a c-Abl-dependent mechanism, wild-type ($Abl^{+/+}$) and c-Abl-deficient ($Abl^{-/-}$) mouse fibroblasts[12] were transfected to express GFP–p73β and then exposed to ionizing radiation: tyrosine phosphorylation occurred on p73β in irradiated $Abl^{+/+}$ but not $Abl^{-/-}$ cells (Fig. 2e); there was no detectable phosphorylation of p73β(Y^{99}-F) in irradiated $Abl^{+/+}$ cells (data not shown). Radiation-induced c-Abl kinase activity is diminished in cells from patients with ataxia telangiectasia (AT)[7,8]. To determine whether tyrosine phosphorylation of p73 is affected in AT cells, we transfected human diploid (HDF) and ATM-deficient[7] AT5 fibroblasts with GFP–p73β. Analysis of anti-GFP immunoprecipitates with anti-P-Tyr indicated that radiation-induced tyrosine phosphorylation of p73β is diminished in AT5 cells relative to control cells (Fig. 2f). Taken together, these results show that c-Abl phosphorylates p73 on Tyr 99 in response to DNA damage.

To determine whether c-Abl affects p73 function, we transfected SAOS2 cells, which are deficient in both p53 (ref. 13) and p73 (ref. 1), with a construct containing the luciferase gene driven by a p53 enhancer from the *MDM2* promoter (mdm2NA-Luc)[14] that had been used previously for p73 transactivation assays[2] (Fig. 3a). Co-transfection of mdm2NA-Luc with vectors expressing wild-type c-Abl or kinase-inactive c-Abl(K-R) had no detectable effect on luciferase activity (Fig. 3a). By contrast, co-transfection of mdm2NA-Luc and the GFP–p73β vector resulted in activation of the luciferase reporter (Fig. 3a). Expression of c-Abl, but not of c-Abl(K-R), enhanced the transactivation function of p73β (Fig. 3a). To assess this role of c-Abl in p73-mediated transactivation, we assayed SAOS2 cell transfectants for induction of p21. As shown previously[15], expression of p73β was associated with increased expression of p21 protein (Fig. 3b). Co-transfection of p73β and c-Abl, but not c-Abl(K-R), strongly induced p21 compared with cells transfected with p73β alone (Fig. 3b). As controls, transfection of c-Abl or c-Abl(K-R) in the absence of p73 had little, if any, effect on p21 expression (Fig. 3b). The finding that transfection of p73β(Y^{99}-F) caused induction of p21 indicated that this mutant has an intact transactivation function (Fig. 3b). However, in contrast to wild-type p73β, co-transfection of c-Abl with p73β(Y^{99}-F) had no detectable effect on the induction of p21 compared with that mediated by p73β(Y^{99}-F) alone (Fig. 3b). These findings show that c-Abl induces the transactivation function of p73 by phosphorylation of Tyr 99.

As transfection of SAOS2 cells with p73 results in the induction of apoptosis[2], we tested whether interaction between c-Abl and p73

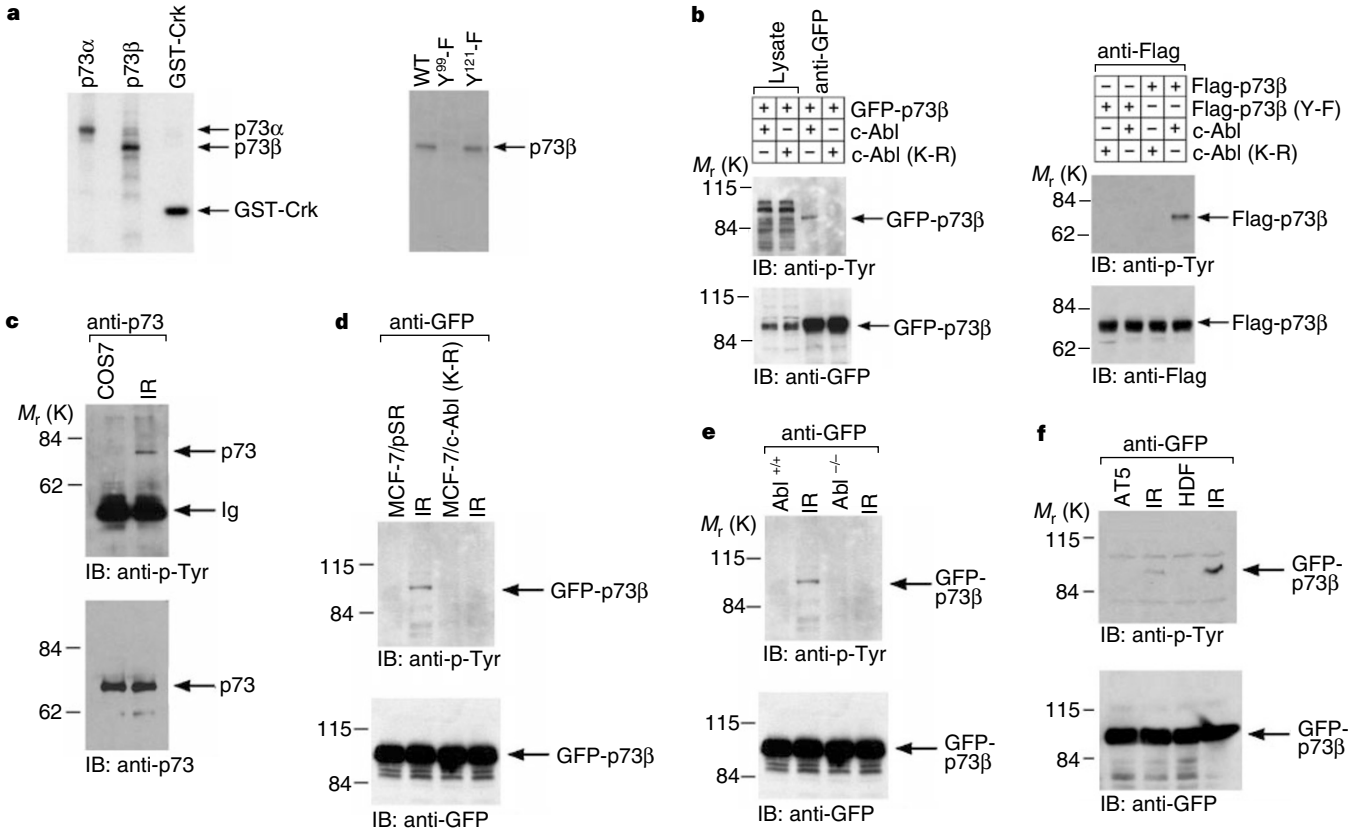

Figure 2 Phosphorylation of p73 by c-Abl. **a**, 293 cells were transfected with Flag–p73α, Flag–p73β, Flag–p73β(Y^{99}-F) or Flag–p73β(Y^{121}-F). Immunopurified proteins were incubated with recombinant c-Abl and [γ-^{32}P]ATP. GST–Crk(120–225) was used as a control. Reaction products were analysed by SDS–PAGE and autoradiography. **b**, 293 cells were transfected with GFP–p73β and c-Abl or c-Abl(K-R) (left). After 48 h, lysates were immunoprecipitated with anti-GFP, and the precipitates immunoblotted with anti-P-Tyr and anti-GFP (right two lanes). Lysates were analysed by immunoblotting (left two lanes). 293 cells were transfected with Flag–p73β, Flag–p73β(Y^{99}-F), c-Abl or c-Abl(K-R) (right). After 48 h, lysates were immunoprecipitated with anti-Flag and the precipitates immunoblotted with anti-P-Tyr and anti-Flag. **c**, COS7 cells were exposed to 20 Gy of ionizing radiation and harvested at 1 h. Anti-p73 immunoprecipitates were immunoblotted with anti-P-Tyr and anti-p73. **d**, MCF-7/pSR and MCF-7/c-Abl(K-R) cells were transfected with GFP–p73β. At 48 h, cells were exposed to 20 Gy ionizing radiation and collected after 1 h for preparation of lysates. Anti-GFP immunoprecipitates were immunoblotted with anti-P-Tyr and anti-GFP. **e**, Wild-type ($Abl^{+/+}$) and $Abl^{-/-}$ fibroblasts were transfected with GFP–p73β. At 48 h, cells were exposed to 20 Gy IR and harvested at 1 h. Anti-GFP immunoprecipitates were immunoblotted with anti-P-Tyr and anti-GFP. **f**, Human diploid fibroblasts (HDF) and AT5 fibroblasts were transfected with GFP–p73β, incubated for 48 h, exposed to 20 Gy IR and then harvested at 1 h. Anti-GFP immunoprecipitates were analysed with anti-P-Tyr and anti-GFP.

© 1999 Macmillan Magazines Ltd

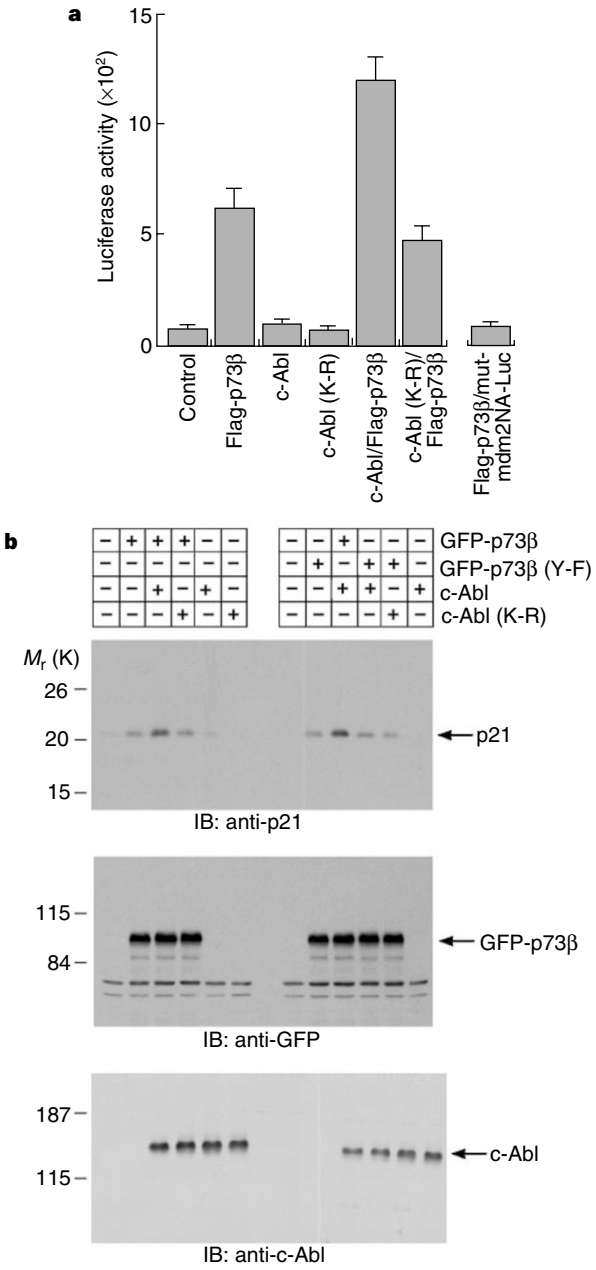

Figure 3 c-Abl induces p73-mediated transactivation. **a**, SAOS2 cells were co-transfected with 0.5 μg p53-enhancer-luciferase plasmid (mdm2NA-Luc) and: (bar 1) 2 μg Flag-pcDNA3 and 2 μg pSR empty vectors; (bar 2) 2 μg Flag-p73β and 2 μg pSR; (bar 3) 2 μg Flag-pcDNA3 and 2 μg pSR-c-*abl*; (bar 4) 2 μg Flag-pcDNA3 and 2 μg pSR-c-*abl*(K-R); (bar 5) 2 μg Flag-p73β and 2 μg c-*abl*; (bar 6) 2 μg Flag-p73β and 2 μg c-*abl*(K-R). SAOS2 cells were also co-transfected with 1 μg p53-enhancer-luciferase plasmid containing a mutated p53 binding site (mut-mdm2NA-Luc), 2 μg Flag-p73β and 2 μg pSR (right bar). Luciferase activity was measured 24 h after transfection and normalized for protein concentration to that for control vector. **b**, SAOS2 cells were transfected with the indicated vectors. Cells were collected at 24 h and their lysates immunoblotted with anti-p21, anti-c-Abl and anti-GFP.

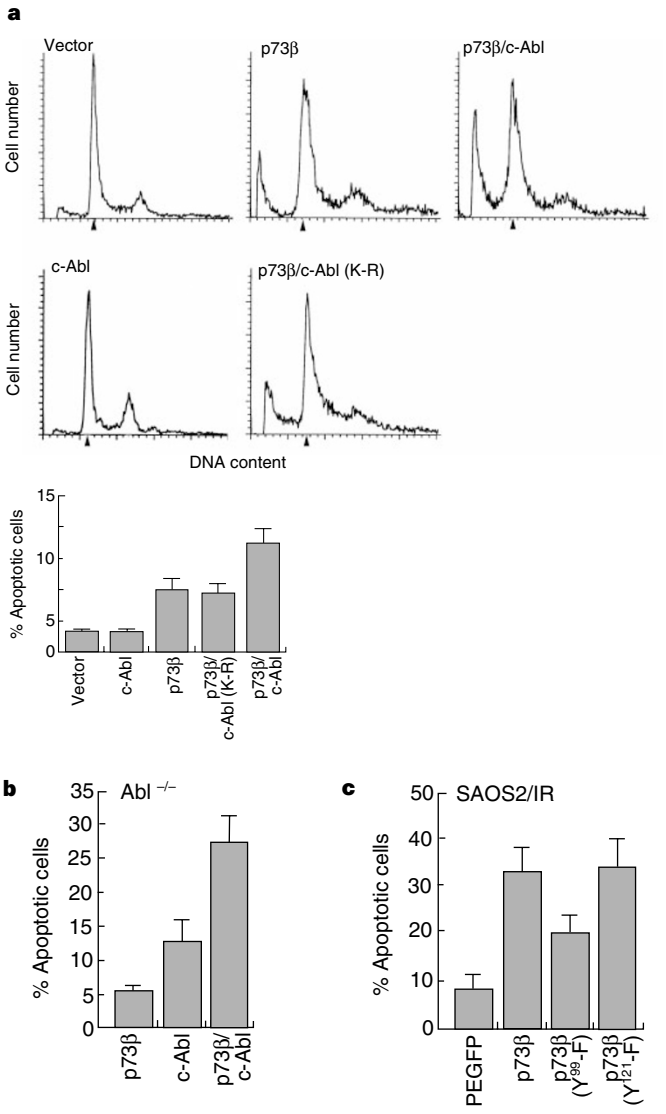

Figure 4 Interaction between c-Abl and p73 contributes to ionizing-radiation-induced apoptosis. **a**, SAOS2 cells were transfected with GFP-p73β, GFP-p73β(Y^{99}-F), c-Abl or c-Abl(K-R). Cells were collected at 48 h and assayed for DNA content (top panels). pEGFP was co-transfected with c-Abl. The results (mean ± s.e. of three experiments) are expressed as the percentage of cells with sub-G1 DNA (bottom panels). **b**, $Abl^{-/-}$ cells were transfected with GFP-p73β, c-Abl or with GFP-p73β and c-Abl. pEGFP was co-transfected with c-Abl. The results (mean ± s.e. of two experiments, each done in duplicate) are expressed as the percentage of cells with sub-G1 DNA. **c**, SAOS2 cells were transfected with GFP, GFP-p73β, GFP-p73β(Y^{99}-F) or GFP-p73β(Y^{121}-F). At 24 h, cells were exposed to 20 Gy IR, collected after an additional 24 h and their DNA content assayed. Results (mean ± s.e. of two experiments, each done in duplicate) are expressed as the percentage of cells with sub-G1 DNA. The percentage of apoptotic cells expressing p73β(Y^{99}-F), compared to p73β or p73β(Y^{121}-F), is significantly different ($P < 0.05$).

affects p73-induced apoptosis. Whereas overexpression of c-Abl in MCF-7 cells and mouse embryo fibroblasts causes apoptosis[4], transfection of the c-Abl vector into SAOS2 cells gave no apoptotic response (Fig. 4a); however, SAOS2 cells transfected to express GFP–p73β showed an increase in the number of cells with sub-G1 DNA content compared with cells expressing empty vector (Fig. 4a). Co-transfection of GFP–p73β and c-Abl(K-R) had little, if any, effect compared with the proportion of apoptotic cells resulting from expression of GFP–p73β alone (Fig. 4a). However, in contrast to the result with GFP–p73β, co-expression of GFP–p73β and c-Abl caused an increase in the number of apoptotic cells (Fig. 4a). To confirm the importance of the interaction between c-Abl and p73 in the induction of apoptosis, we co-transfected $Abl^{-/-}$ cells with GFP–p73β and either empty vector or c-Abl: we found that overexpression of GFP–p73β had little effect on apoptosis of $Abl^{-/-}$ cells (Fig. 4b). Co-transfection of GFP–p73β and c-Abl, however, gave a substantial increase in the percentage of cells with sub-G1 DNA content compared with transfection with c-Abl alone (Fig. 4b). The

© 1999 Macmillan Magazines Ltd

finding that c-Abl induces the apoptotic function of p73 suggests that p73 may be an effector of a c-Abl-dependent apoptotic response to DNA damage. To determine whether p73 is involved in apoptosis induced by ionizing radiation, we transfected SAOS2 cells to make them overexpress GFP–p73β, p73β(Y^{99}-F) or p73β(Y^{121}-F), and then irradiated them. There was little apoptosis in irradiated cells expressing the empty vector, whereas cells expressing p73β or p73β(Y^{121}-F) showed an increase in the number of cells with a sub-G1 DNA content (Fig. 4c). By contrast, overexpression of p73β(Y^{99}-F) blocked in part the apoptotic response to ionizing radiation (Fig. 4c). These findings collectively support a model in which c-Abl-mediated phosphorylation of p73 contributes to DNA-damage-induced apoptosis.

The apoptotic response of irradiated cells has been associated with expression of wild-type p53 (refs 16–18). c-Abl interacts with p53 in irradiated cells, but does not phosphorylate it, and contributes to radiation-induced G1 arrest by a p53-dependent mechanism[11]. In contrast, c-Abl regulates DNA-damage-induced apoptosis predominantly by a p53-independent mechanism[4]. Our results support a model in which c-Abl regulates the p53-related p73 protein to induce DNA-damage-mediated apoptosis. Although it is known that p53 protein accumulates as a result of genotoxic stress[19] and p73 does not[1,2], our results show that p73 is phosphorylated by a c-Abl-dependent mechanism in the DNA-damage response. The functional significance of the c-Abl/p73 interaction is supported by our findings that active c-Abl, and not inactive c-Abl(K-R), induces both p73-mediated transactivation and apoptosis. From our demonstration that preventing interaction between c-Abl and p73 also prevents radiation-induced apoptosis, we conclude that p73 is regulated by c-Abl in the DNA-damage response. We have provided evidence that p73 is activated by c-Abl kinase and that it participates in the apoptotic response to DNA damage. □

Methods

Cell culture. COS7, 293, MCF-7/pSR and MCF-7/c-Abl(K-R)[4] cells were cultured in Dulbecco's modified Eagle's medium containing 10% heat-inactivated fetal bovine serum (HI-FBS), 2 mM L-glutamine, 10 units ml^{-1} penicillin and 100 μg ml^{-1} streptomycin. SAOS2 cells were grown in McCoy's 5a medium containing 10% HI-FBS, 2 mM L-glutamine, 10 units ml^{-1} penicillin and 100 μg ml^{-1} streptomycin. Wild-type ($Abl^{+/+}$), c-Abl-deficient ($Abl^{-/-}$), human diploid (GM00637F) and ATM-deficient AT5BIVA fibroblasts were all grown as described[3,7,20]. Vectors were introduced into cells by using the Effectene transfection kit (Qiagen). Cells were treated with ionizing radiation at room temperature with a Gammacell 1000 (Atomic Energy of Canada) and a ^{137}Cs source emitting at a fixed rate of 0.21 Gy min^{-1}.

Plasmid construction. Vectors expressing GFP-p73α and GFP-p73β were generated by subcloning human p73α or p73β cDNAs[1] into pEGFP (Clontech). Vectors expressing Flag–p73α, Flag–p73β, Flag–p73β TAD (amino acids 1–125), Flag–p73β DBD (amino acids 128–313) and Flag–p73β OD (amino acids 311–499) were generated by subcloning full-length PCR-generated products from the p73α and p73β cDNAs[1] into Flag-tagged pcDNA3. Vectors expressing Flag–p73β(Y^{99}-F) and Flag-p73β(Y^{121}-F) were prepared by site-directed mutagenesis.

Immunoprecipitation and immunoblot analysis. Cell lysates were prepared in lysis buffer containing 0.5% Nonidet P-40 and immunoprecipitated as described[11] with anti-c-Abl (Ab-3; Oncogene Science), anti-RPA70 (Ab-1; Oncogene Science), anti-p73 (rabbit antiserum against p73; amino acids SAATPNLGPVGPGML) or anti-GFP (Clontech). Proteins were separated on SDS–polyacrylamide gels and western-blotted with anti-p73, anti-c-Abl, anti-RPA70, anti-P-Tyr (4G10; Upstate Biotechnology Inc.) or anti-p21 (Abl-1, Oncogene Science) antibodies.

Fusion-protein binding assays. Purified GST, GST–Abl SH3 (ref. 21) and GST–Abl SH2 (amino acids 115–213) proteins (5 μg) were incubated with ^{35}S-labelled Flag–p73α or Flag–p73β. GST–Abl SH3 was incubated with ^{35}S-labelled Flag–p73β TAD, Flag–p73β DBD or Flag–p73β OD and the adsorbates analysed by SDS–PAGE and autoradiography.

***In vitro* kinase assays.** Kinase-active c-Abl or kinase-inactive c-Abl(K-R) purified from baculovirus was incubated with immunoaffinity-purified Flag–p73α, Flag–p73β, Flag–p73β(Y^{99}-F), Flag–p73β(Y^{121}-F) or a GST–Crk control, and [γ-^{32}P]ATP in kinase buffer (20 mM HEPES, pH 7.5, 1 mM dithiothreitol, 10 mM $MgCl_2$) for 15 min at 30 °C. Phosphorylated proteins were separated by SDS–PAGE and analysed by autoradiography.

Luciferase assays. Transient transfections of SAOS2 cells with mdm2NA-Luc[14] were done with the Effectene transfection kit and cells were collected 24 h after transfection. Luciferase was assayed with an enhanced luciferase assay kit (1800K, Analytical Luminescence).

Apoptosis assays. DNA content was assessed by staining ethanol-fixed cells with propidium iodide and monitoring by FACScan (Becton-Dickinson). Numbers of GFP-positive cells with sub-G1 DNA content were determined with a MODFIT LT program.

Received 6 May; accepted 19 May 1999.

1. Kaghad, M. *et al.* Monoallelically expressed gene related to p53 at 1p36, a region frequently deleted in neuroblastoma and other human cancers. *Cell* **90,** 809–819 (1997).
2. Jost, C. A., Marin, M. C. & Kaelin, W. G. Jr p73 is a human p53-related protein that can induce apoptosis. *Nature* **389,** 191–193 (1997).
3. Kharbanda, S. *et al.* Activation of the c-Abl tyrosine kinase in the stress response to DNA-damaging agents. *Nature* **376,** 785–788 (1995).
4. Yuan, Z.-M. *et al.* Regulation of DNA-damage-induced apoptosis by the c-Abl tyrosine kinase. *Proc. Natl Acad. Sci. USA* **94,** 1437–1440 (1997).
5. Kharbanda, S. *et al.* c-Abl activation regulates induction of the SEK1/stress activated protein kinase pathway in the cellular response to 1-β-D-arabinofuranosylcytosine. *J. Biol. Chem.* **270,** 30278–30281 (1995).
6. Kharbanda, S. *et al.* Functional interaction of DNA-PK and c-Abl in response to DNA damage. *Nature* **386,** 732–735 (1997).
7. Shafman, T. *et al.* Interaction between ATM protein and c-Abl in response to DNA damage. *Nature* **387,** 520–523 (1997).
8. Baskaran, R. *et al.* Ataxia telangiectasia mutant protein activates c-Abl tyrosine kinase in response to ionizing radiation. *Nature* **387,** 516–519 (1997).
9. Sawyers, C. L., McLaughlin, J., Goga, A., Havilik, M. & Witte, O. The nuclear tyrosine kinase c-Abl negatively regulates cell growth. *Cell* **77,** 121–131 (1994).
10. Marin, M. C. *et al.* Viral oncoproteins discriminate between p53 and the p53 homolog p73. *Mol. Cell. Biol.* **18,** 6316–6324 (1998).
11. Yuan, Z. M. *et al.* Role for the c-Abl tyrosine kinase in the growth arrest response to DNA damage. *Nature* **382,** 272–274 (1996).
12. Tybulewicz, V. L. J., Crawford, C. E., Jackson, P. K., Bronson, R. T. & Mulligan, R. C. Neonatal lethality and lymphopenia in mice with a homozygous disruption of the c-*abl* proto-oncogene. *Cell* **65,** 1153–1163 (1991).
13. Diller, L. *et al.* p53 functions as a cell cycle control protein in osteosarcomas. *Mol. Cell. Biol.* **10,** 5772–5781 (1990).
14. Barak, Y., Gottlieb, E., Juven-Gershon, T. & Oren, M. Regulation of mdm2 expression by p53: alternative promoters produce transcripts with nonidentical translation potential. *Genes Dev.* **8,** 1739–1749 (1994).
15. Zhu, J., Jiang, J., Zhou, W. & Chen, X. The potential tumor suppressor p73 differentially regulates cellular p53 target genes. *Cancer Res.* **58,** 5061–5065 (1998).
16. Clarke, A. R. *et al.* Thymocyte apoptosis induced by p53-dependent and independent pathways. *Nature* **362,** 849–852 (1993).
17. Lowe, S. W., Schmitt, E. M., Smith, S. W., Osborne, B. A. & Jacks, T. p53 is required for radiation-induced apotosis in mouse thymocytes. *Nature* **362,** 847–849 (1993).
18. Lowe, S. W., Ruley, H. E., Jacks, T. & Housman, D. E. p53-dependent apoptosis modulates the cytotoxicity of anticancer agents. *Cell* **74,** 957–967 (1993).
19. Kastan, M. B., Onyekwere, O., Sidransky, D., Vogelstein, B. & Craig, R. W. Participation of p53 protein in the cellular response to DNA damage. *Cancer Res.* **51,** 6304–6311 (1991).
20. Luo, C. M. *et al.* High frequency and error-prone DNA recombination in ataxia telangiectasia cell lines. *J. Biol. Chem.* **271,** 4497–4503 (1996).
21. Ren, R., Ye, Z.-S. & Baltimore, D. Abl protein-tyrosine kinase selects the Crk adapter as a substrate using SH3-binding sites. *Genes Dev.* **8,** 783–795 (1994).

Correspondence and requests for materials should be addressed to D.K. (e-mail: donald_kufe@dfci.harvard.edu).

correction

p73 is a human p53-related protein that can induce apoptosis

Christine A. Jost, Maria C. Marin & William G. Kaelin Jr

Nature **389,** 191–194 (1999)

It has come to *Nature's* attention that the title of this Letter is misleading. In fact, the p73 cDNA sequence used in this work was of simian, not human, origin.

The GenBank database accession number for this African green monkey p73 sequence is Y11419. □

© 1999 Macmillan Magazines Ltd

six independent founder mice (FvB/N × C57BL/6) were obtained from 18 pups that were born. The *cre* gene was modified to contain the nuclear localization sequence of the SV40 large T antigen by PCR and cloned into the *Bam*HI site of p687 (ref. 10) and the *Eco*RI fragment was used to generate transgenic mice. Of the ten pups that were born, four carried the transgene. The founder mice were bred to generate transgenic lines.

Immunization and infection. Cohorts of transgenic and non-transgenic littermate control mice were immunized intraperitoneally with 100 μg KLH emulsified in Ribi adjuvant. For LCMV infection, mice were injected intraperitoneally with 5×10^4 PFU of the Armstrong strain of LCMV. Spleens were collected and analysed by frozen sectioning and FACS analysis at 8, 30, 60 and 90 days post-infection.

Cytotoxicity assay. CTL assays were performed as described[2]. Sorted $CD8^+$ $PLAP^+$ and $PLAP^-$ T cells ($H\text{-}2^{b/q}$, $H\text{-}2^b$ or $H\text{-}2^q$) were plated in triplicate to achieve the desired effector/target ratio along with ^{51}Cr-labelled uninfected or LCMV-infected target cells. MC57G ($H\text{-}2^b$) and CRL-2110 ($H\text{-}2^q$) (ATCC) were used as target cells. Following 6 h incubation at 37 °C the supernatant was collected and counted. Percent specific lysis was calculated as 100 × [(experimental c.p.m. − spontaneous c.p.m.) / (maximum release − spontaneous release)].

Secondary bulk CTL assay. $CD8^+$ $PLAP^+$ and $PLAP^-$ T cells were purified by FACS from mice infected eight days earlier with LCMV. 10^6 sorted cells ($CD8^+$ $PLAP^+$ and $PLAP^-$) were co-cultured with 8×10^5 irradiated (1,200 rad) syngeneic spleen cells, 2×10^5 irradiated LCMV-infected, thioglycollate-induced PEC and IL-2 (20 units) in a 200 μl volume. After six days of incubation at 37 °C, their cytotoxicity was tested in a 6–8-h ^{51}Cr-release assay.

Adoptive transfer. Adoptive transfer and viral challenge were done as described[25]. Briefly, $CD8^+$ $PLAP^+$ and $PLAP^-$ T cells were isolated by FACS from LCMV-immune doubly transgenic mice (infected >1 month earlier with LCMV Arm). The sorted cells were injected into the lateral tail vein of syngeneic naive recipients that had been irradiated 1 day earlier (600 rad). Each recipient received 2×10^5 $PLAP^+$ or $PLAP^-$ $CD8^+$ T cells. The day after adoptive transfer, recipient mice were challenged with a single i.v. injection of 2×10^6 PFU of clone 13 LCMV. Eight days after the viral challenge, the spleens were removed, homogenized and titred for LCMV by plaquing on Vero cells[30].

Received 25 January; accepted 9 April 1999.

1. Hou, S., Hyland, L., Ryan, K. W., Portner, A. & Doherty, P. C. Virus-specific $CD8^+$ T-cell memory determined by cloning burst size. *Nature* **369,** 652–654 (1994).
2. Welsh, R. M. *et al*. Alpha beta and gamma delta T-cell networks and their roles in natural resistance to viral infections. *Immuno. Rev.* **159,** 79–93 (1997).
3. Kundig, T. M. *et al*. On T cell memory: arguments for antigen dependence. *Immun. Rev.* **150,** 63–90 (1996).
4. Mullbacher, A. & Flynn, K. Aspects of cytotoxic T cell memory. *Immun. Rev.* **150,** 113–127 1996).
5. Tough, D. F. & Sprent, J. Lifespan of lymphocytes. *Immun. Res.* **14,** 1–12 (1995).
6. Swain, S. L. *et al*. From naive to memory T cells. *Immun. Rev.* **150,** 143–167 (1996).
7. Doherty, P. C., Topham, D. J. & Tripp, R. A. Establishment and persistence of virus-specific $CD4^+$ and $CD8^+$ T cell memory. *Immun. Rev.* **150,** 23–44 (1996).
8. Lasko, M. Targeted oncogene activation by site-specific recombination in transgenic mice. *Proc. Natl Acad. Sci. USA* **89,** 6232–6236 (1992).
9. Cepko, C., Ryder, E. F., Austin, C. P., Walsh, C. & Fekete, D. M. Lineage analysis using retrovirus vectors. *Methods Enzymol.* **254,** 387–419 (1995).
10. Hanson, R. D., Sclar, G. M., Kanagawa, O. & Ley, T. J. The 5′-flanking region of the human CGL-1/granzyme B gene targets expression of a reporter gene to activated T-lymphocytes in transgenic mice. *J. Biol. Chem.* **266,** 24433–24438 (1991).
11. Zhumabekov, T., Corbella, P., Tolaini, M. & Kioussis, D. Improved version of a human CD2 minigene based vector for T cell-specific expression in transgenic mice. *J. Biol. Chem.* **266,** 24433–24438 (1991).
12. Williams, A. F., Barclay, A. N., Clark, S. J., Paterson, D. J. & Willis, A. C. Similarities in sequences and cellular expression between rat CD2 and CD4 antigens. *J. Exp. Med.* **165,** 368–380 (1987).
13. Wotton, D., Flanagan, B. F. & Owen, M. J. Chromatin configuration of the human CD2 gene locus during T-cell development. *Proc. Natl Acad. Sci. USA* **86,** 4195–4199 (1989).
14. Nagy, A. *et al*. Multipurpose gene alterations from a single targeting vector: dissecting the role of N-myc in development. *Curr. Biol.* **8,** 661–664 (1998).
15. Castan, J., Tenner, R. K., Racz, P., Fleischer, B. & Broker, B. M. Accumulation of CTLA-4 expressing T lymphocytes in the germinal centres of human lymphoid tissues. *Immunology* **90,** 265–271 (1997).
16. Zheng, B., Han, S., Zhu, Q., Goldsby, R. & Kelsoe, G. Alternative pathways for the selection of antigen-specific peripheral T cells. *Nature* **384,** 263–266 (1996).
17. Fuller, K. A., Kanagawa, O. & Nahm, M. H. T cells within germinal centers are specific for the immunizing antigen. *J. Immunol.* **151,** 4505–4512 (1993).
18. Gulbranson, J. A. & MacLennan, I. Sequential antigen-specific growth of T cells in the T zones and follicles in response to pigeon cytochrome c. *Eur. J. Immunol.* **26,** 1830–1837 (1996).
19. Ahmed, R., Byrne, J. A. & Oldstone, M. B. Virus specificity of cytotoxic T lymphocytes generated during acute lymphocytic choriomeningitis virus infection: role of the H-2 region in determining cross-reactivity for different lymphocytic choriomeningitis virus strains. *J. Virol.* **51,** 34–41 (1984).
20. Jamieson, B. D. & Ahmed, R. T cell memory. Long-term persistence of virus-specific cytotoxic T cells. *J. Exp. Med.* **169,** 1993–2005 (1989).
21. Selin, L. K., Nahill, S. R. & Welsh, R. M. Cross-reactivities in memory cytotoxic T lymphocyte recognition of heterologous viruses. *J. Exp. Med.* **179,** 1933–1943 (1994).
22. Zimmerman, C., Brduscha, R. K., Blaser, C., Zinkernagel, R. M. & Pircher, H. Visualization, characterization, and turnover of $CD8^+$ memory T cells in virus-infected hosts. *J. Exp. Med.* **183,** 1367–1375 (1996).
23. Nahill, S. R. & Welsh, R. M. High frequency of cross-reactive cytotoxic T lymphocytes elicited during the virus-induced polyclonal cytotoxic T lymphocyte response. *J. Exp. Med.* **177,** 317–327 (1993).
24. Yang, H. Y., Dundon, P. L., Nahill, S. R. & Welsh, R. M. Virus-induced polyclonal cytotoxic T lymphocyte stimulation. *J. Immunol.* **142,** 1710–1718 (1989).
25. Lau, L. L., Jamieson, B. D., Somasundaram, T. & Ahmed, R. Cytotoxic T-cell memory without antigen. *Nature* **369,** 648–652 (1994).
26. Ahmed, R. & Gray, D. Immunological memory and protective immunity: understanding their relation. *Science* **272,** 54–60 (1996).
27. Zinkernagel, R. M. *et al*. On immunological memory. *Annu. Rev. Immunol.* **14,** 333–367 (1996).
28. Murali, K. K. *et al*. Counting antigen-specific CD8 T cells: a reevaluation of bystander activation during viral infection. *Immunity* **8,** 177–187 (1998).
29. Butz, E. A. & Bevan, M. J. Massive expansion of antigen-specific $CD8^+$ T cells during an acute virus infection. *Immunity* **8,** 167–175 (1998).
30. Ahmed, R., Salmi, A., Butler, L. D., Chiller, J. M. & Oldstone, M. B. A. Selection of genetic variants of lymphocytic choriomeningitis virus in spleens of persistently infected mice: role in suppression of cytotoxic T lymphocyte response and viral persistence. *J. Exp. Med.* **60,** 521–540 (1984).

Acknowledgements. We thank C. Roman, I. Stancovski, S. Cherry, K. Alexandroplous, M. Scott, G. Kelsoe, R. Welsh, L. Selin, R. Ahmed and members of the Baltimore laboratory for useful discussions. We also thank T. Ley for p687 plasmid; R. Welsh, R. Ahmed and J. Carlos de la Torre for LCM viral stocks; D. Kioussis for the VahCD2 transgenic construct; M. Brasch for pBS185 and pBS302 plasmids; and A. Nagy for the hCMV-Cre transgenic mice. J.J. Thanks H. Rayburn and W. Sha for teaching him pronuclear injection and transgenesis, and M. Scott for help with adoptive transfers. J.J. was a recipient of a postdoctoral fellowship from the Helen Hay Whitney foundation and is currently a special fellow of the Leukemia Society of America.

Correspondence and requests for materials should be addressed to D.B. (e-mail: baltimo@caltech.edu).

Regulation of endothelium-derived nitric oxide production by the protein kinase Akt

David Fulton*, Jean-Philippe Gratton*, Timothy J. McCabe*, Jason Fontana*, Yasushi Fujio†, Kenneth Walsh†, Thomas F. Franke‡, Andreas Papapetropoulos* & William C. Sessa*

* *Department of Pharmacology and Molecular Cardiobiology Program, Boyer Center for Molecular Medicine, Yale University School of Medicine, New Haven, Connecticut 06536, USA*
† *Cardiovascular Research, St. Elizabeth's Medical Center, Boston, Massachusetts 02135, USA*
‡ *Department of Pharmacology, Columbia University, New York, New York 10032, USA*

Endothelial nitric oxide synthase (eNOS) is the nitric oxide synthase isoform responsible for maintaining systemic blood pressure, vascular remodelling and angiogenesis[1–4]. eNOS is phosphorylated in response to various forms of cellular stimulation[5–7], but the role of phosphorylation in the regulation of nitric oxide (NO) production and the kinase(s) responsible are not known. Here we show that the serine/threonine protein kinase Akt (protein kinase B) can directly phosphorylate eNOS on serine 1179 and activate the enzyme, leading to NO production, whereas mutant eNOS (S1179A) is resistant to phosphorylation and activation by Akt. Moreover, using adenovirus-mediated gene transfer, activated Akt increases basal NO release from endothelial cells, and activation-deficient Akt attenuates NO production stimulated by vascular endothelial growth factor. Thus, eNOS is a newly described Akt substrate linking signal transduction by Akt to the release of the gaseous second messenger NO.

The Akt proto-oncogene is an important regulator of various cellular processes including glucose metabolism and cell survival[8,9]. Activation of receptor tyrosine kinases and G-protein-coupled receptors, and stimulation of cells by mechanical forces, can lead to the phosphorylation and activation of Akt[10–12]. Akt can then phosphorylate substrates such as glycogen synthase kinase-3, Bad and caspase-9, resulting in protein inactivation, or 6-phospho-fructo-2-kinase, resulting in protein activation[10,13]. The relationships between activation of Akt, its downstream effectors and the production of soluble second messengers are not well understood.

© 1999 Macmillan Magazines Ltd

eNOS is the nitric oxide synthase (NOS) isoform that produces endothelium-derived NO. Treatment of endothelial cells with vascular endothelial growth factor (VEGF) or insulin stimulates the production of NO by a phosphatidylinositol-3-OH-kinase (PI(3)K)-dependent mechanism[14,15]. Wortmannin and LY294002, two structurally dissimilar inhibitors of PI(3)K, partially block NO release. VEGF also stimulates the Ras pathway; inhibition of Ras signalling blocks extracellular-signal-related-kinase (ERK)-1/2 activation, but not VEGF-stimulated NO production, indicating that there may be a link between growth factor signalling through PI(3)K and eNOS[16].

To investigate whether Akt, a downstream effector of PI(3)K, could directly influence the production of NO, COS-7 cells (which do not express NOS) were co-transfected with eNOS and wild-type

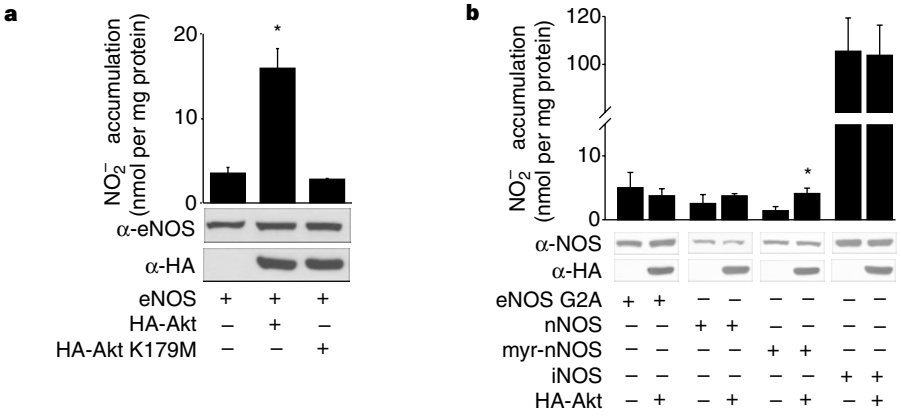

Figure 1 Wild-type Akt, but not kinase-inactive Akt, increases NO release from cells expressing membrane-associated eNOS. **a**, COS cells were transfected with plasmids for eNOS, with or without Akt or kinase-inactive Akt (K179M). The production of NO (assayed as NO_2^-) was determined by chemiluminescence. **b**, COS cells were transfected with various NOS plasmids as above. In both **a** and **b**, values for NO_2^- production were subtracted from levels obtained from cells transfected with the β-galactosidase cDNA only. The insets show the expression of proteins in total cell lysates. Data were mean ± s.e.m., $n = 3$–7 experiments; asterisk denotes $P < 0.05$.

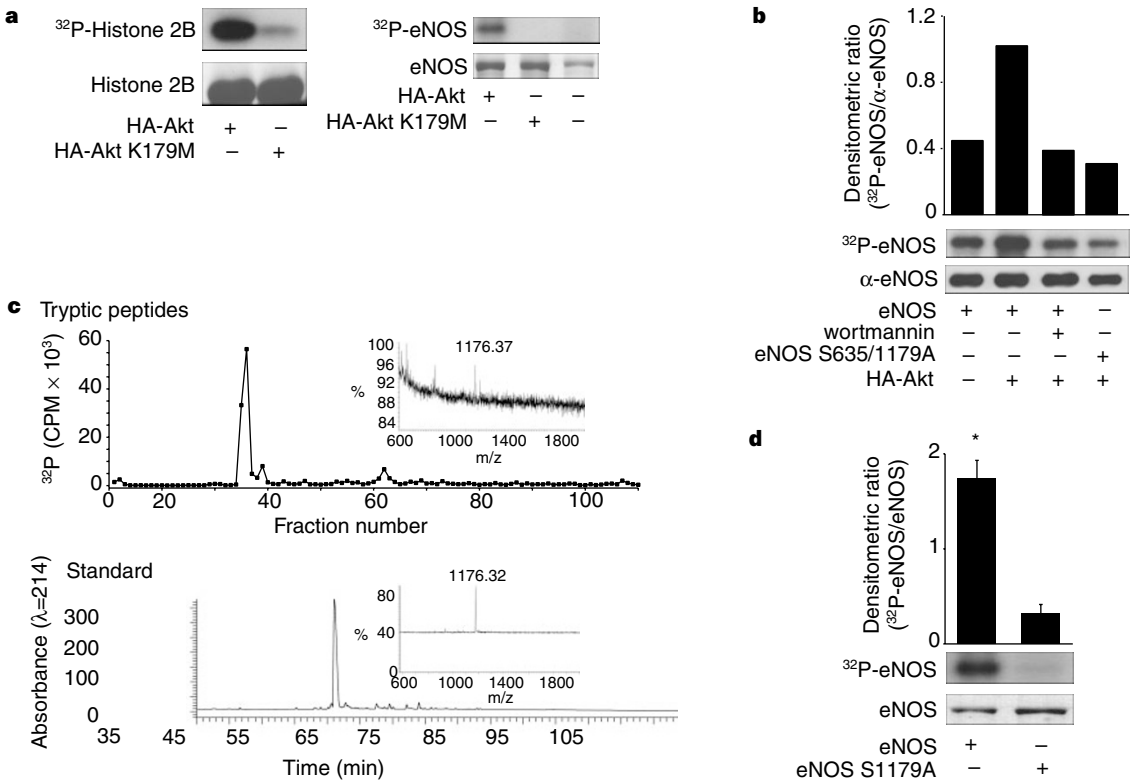

Figure 2 Phosphorylation of eNOS by active Akt *in vitro* and *in vivo*. **a**, COS cells were transfected with HA–Akt or HA–Akt(K179M) and lysates were immunoprecipitated and placed into an *in vitro* kinase reaction with histone 2B (25 μg) or recombinant eNOS (3 μg) as substrates. Top panel: incorporation of ^{32}P into the substrates; Bottom panel: amount of substrate by Coomassie staining of the gel. **b**, ^{32}P-labelled wild-type or double-serine mutant of eNOS (eNOS S635/1179A) was affinity purified from transfected COS cells and subjected to autoradiography (upper panel) or western blotting (lower panel). The histogram shows the relative amount of labelled protein to the amount of immunoreactive eNOS in the gel. **c**, Labelled eNOS was digested with trypsin and peptides separated by RP-HPLC. The upper panel shows a predominant labelled tryptic peptide that co-migrates with the unlabelled synthetic phosphopeptide standard (bottom panel). Insets: linear mode MS of labelled peptide (top) and phosphopeptide standard showing identical mass ions (bottom). **d**, Recombinant wild-type eNOS or eNOS S1179A were purified and equal amounts (2.4 μg) placed into an *in vitro* kinase reaction with recombinant Akt (see Methods). Top panel: the incorporation of ^{32}P into eNOS; bottom panel; amount of substrate by Coomassie staining of the gel. Histogram ($n = 3$) reflects the relative amount of labelled eNOS to the mass of eNOS (Coomassie) in the *in vitro* kinase reaction.

© 1999 Macmillan Magazines Ltd

Akt (HA–Akt) or kinase-inactive Akt (HA–Akt K179M), and the accumulation of nitrite (NO_2^-) was measured by NO-specific chemiluminescence. Transfection of eNOS results in increased NO_2^- accumulation, which is markedly enhanced by co-transfection of wild-type Akt, but not the kinase-inactive variant (Fig. 1a). Identical results were obtained using cyclic GMP (cGMP) as a bioassay for biologically active NO. Transfection of a constitutively active form of Akt (myr-Akt) increases cGMP accumulation (assayed in COS cells) from 5.5 ± 0.8 to 11.6 ± 0.9 pmol cGMP per mg protein (in cells transfected with eNOS alone or eNOS with myr-Akt, respectively) whereas the kinase-inactive Akt did not influence cGMP accumulation (5.8 ± 0.8 pmol cGMP, $n = 4$ experiments). Under these experimental conditions, Akt was catalytically active, as determined by western blotting with a phospho-Akt-specific antibody (which recognizes serine 473; data not shown) and Akt activity assays (see Fig. 2a). Equal levels of eNOS and Akt were expressed in COS cell lysates (Fig. 1), indicating that Akt modulates eNOS, thereby increasing NO production under basal conditions.

eNOS is a dually acylated peripheral membrane protein that targets into the Golgi region and plasma membrane of endothelial cells[17–19]; compartmentalization is required for efficient production of NO in response to agonist challenge[20–22]. To test whether eNOS activation by Akt requires membrane compartmentalization, we co-transfected COS-7 cells with complementary DNAs for Akt and a myristoylation, palmitoylation-defective mutant of eNOS (G2A eNOS); we then quantified the release of NO. Akt did not activate the non-acylated form of eNOS (Fig. 1b), indicating that compartmentalization of both proteins to the membrane is required for their functional interaction[10]. Next, we tested whether Akt could activate two structurally similar but distinct soluble NOS isoforms, neuronal NOS and inducible NOS (nNOS and iNOS, respectively). Co-transfection of Akt with nNOS and iNOS did not result in a further increase in NO release, demonstrating the specificity of Akt for eNOS. However, the addition of an N-myristoylation site to nNOS, to enhance its interactions with biological membranes, results in Akt stimulation of nNOS in a manner analogous to that seen with eNOS, indicating that both isoforms may be susceptible to activation by Akt when anchored to the membrane.

The above data indicate that Akt, perhaps by phosphorylation of eNOS, can modulate NO release from intact cells. Indeed, two putative Akt phosphorylation motifs (RXRXXS/T) are present in eNOS (serines 635 and 1179 in bovine eNOS; serines 633 and 1177 in human eNOS) and one motif is present in nNOS (serines 1412 in rat and 1415 in human nNOS), with no obvious motifs found in iNOS. To test whether eNOS is a potential substrate for Akt phosphorylation *in vitro*, we transfected COS cells with HA–Akt or HA–Akt (K179M), and assessed kinase activity using recombinant eNOS as a substrate. The active kinase phosphorylates histone 2B and eNOS (Fig. 2a; 69.3 ± 2.9 and 115.4 ± 3.8 pmol of ATP per nmol substrate, respectively; $n = 3$), whereas the inactive Akt did not significantly increase histone or eNOS phosphorylation. To investigate whether the putative Akt phosphorylation sites in eNOS were responsible for the incorporation of ^{32}P, the two serines were mutated to alanine residues and the ability of Akt to stimulate wild-type and mutant eNOS phosphorylation was examined in intact COS cells. We labelled transfected cells with ^{32}P-orthophosphate and partially purified eNOS by ADP-sepharose affinity chromatography, and quantified the phosphorylation state and protein levels. Co-expression of Akt results in a twofold enhancement in the phosphorylation of eNOS relative to non-stimulated cells (Fig. 2b). Pretreatment of eNOS/Akt-transfected cells with wortmannin abolished the Akt-induced increase in phosphorylation. Moreover, mutation of serines 635 and 1179 to alanine residues abolished Akt-dependent phosphorylation of eNOS, indicating that these residues could serve as potential phosphorylation sites in intact cells. To directly identify the residues phosphorylated by Akt, we incubated wild-type eNOS with immunopurified Akt and determined the sites of phosphorylation by high-performance liquid chromatography followed by matrix-assisted laser desorption ionization mass spectrometry (MALDi-MS). The primary ^{32}P-labelled tryptic phos-

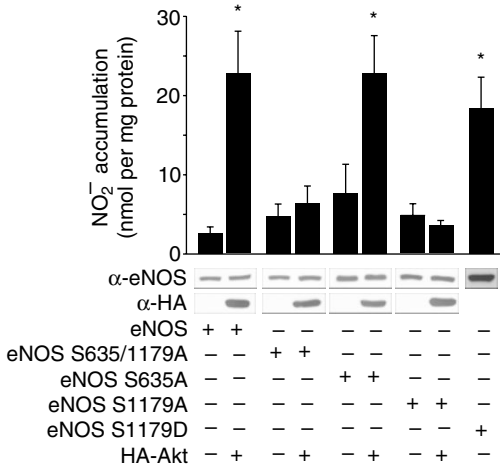

Figure 3 Evidence that Ser 1179 is functionally important for Akt-stimulated NO release. COS cells were transfected with plasmids for wild-type eNOS or eNOS mutants, in the absence or presence of Akt, and the expression of the proteins and production of NO (assayed as NO_2^-) were determined. Constructs with the S1179A mutation were not activated by Akt; the S1179D mutation resulted in a gain of function. Data are mean ± s.e.m. of 4–7 experiments; asterisks represent significant differences ($P < 0.05$).

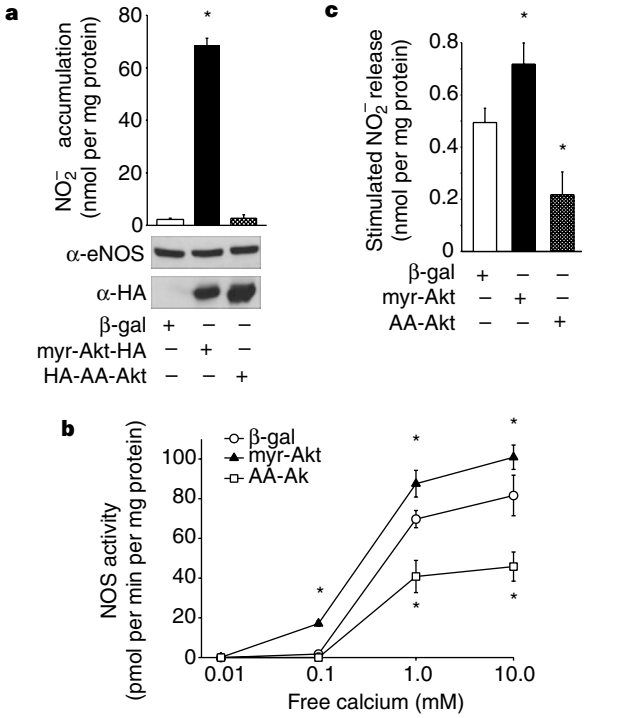

Figure 4 Akt regulates the basal and stimulated production of NO in endothelial cells. **a**, BLMVEC were infected with adenoviral constructs (β-gal as control, myr-Akt and AA-Akt) and the amount of NO_2^- produced over 24 h was determined ($n = 3$). Inset: expression of eNOS and Akt. **b**, Lysates from adenovirus-infected BLMVEC were examined for NOS activity. Equal amounts of protein (50 μg) were incubated with various concentrations of free calcium, and the NOS activity was determined ($n = 3$ experiments). **c**, BLMVEC were infected with adenoviruses as above followed by stimulation with VEGF (40 ng per ml) for 30 min and NO_2^- release was quantified by chemiluminescence. Data are presented as VEGF-stimulated release of NO_2^- after subtraction of basal levels; mean ± s.e.m., $n = 4$; asterisks represent significant differences ($P < 0.05$).

© 1999 Macmillan Magazines Ltd

phopeptide co-elutes with a synthetic phosphopeptide (amino acids 1177–1185 with phosphoserine at position 1179) and has the identical mass ion as determined by linear mode MS (Fig. 2c). Using reflectron mode MALDi-MS monitoring, both the labelled tryptic peptide and the standard phosphopeptide demonstrated a loss of H_3PO_4, indicating that the tryptic peptide was phosphorylated. In addition, mutation of Ser 1179 to alanine markedly reduces Akt-dependent phosphorylation of eNOS compared with the wild-type protein (Fig. 2d). Identical results were obtained using peptides (amino acids 1174–1194) derived from wild-type or eNOS S1179A as substrates for recombinant Akt (the wild-type peptide incorporated 24.6 ± 3.7 nmol phosphate per mg compared to the alanine mutant peptide, which incorporated 0.22 ± 0.02 nmol phosphate per mg; $n = 5$). These data show that eNOS is a substrate for Akt and that the primary site of phosphorylation is serine 1179.

Next we examined the functional significance of the putative Akt phosphorylation site at Ser 635 and the identified site at Ser 1179. Transfection of COS cells with the double mutant eNOS S635/1179A abolishes Akt-dependent NO release. Mutation of Ser 635 to alanine did not attenuate NO release, whereas eNOS S1179A abolishes Akt-dependent activation of eNOS (Fig. 3). These results indicate that Ser 1179 is functionally important for NO release. Mutation of Ser 1179 into aspartic acid (eNOS S1179D), to substitute for the negative charge afforded by the addition of phosphate, partially mimics the activation state induced by Akt. All site-directed mutants were amply expressed (see inset western blots) and retained NOS catalytic activity in cell lysates (in COS cells transfected with eNOS only, NOS activity was 85.3 ± 27.0, 71.9 ± 2.9, 80.8 ± 23.2 and 131.8 ± 36.7 pmol L-citrulline generated per mg protein from lysates of COS cells expressing wild-type, S1179A, S635/1179A and S1179D eNOS, respectively; $n = 3$ experiments).

To test whether Akt mediates NO release from endothelial cells, we infected bovine lung microvascular endothelial cells (BLMVEC) with adenoviruses expressing activated Akt (myr-Akt), activation-deficient Akt (AA-Akt) or β-galactosidase (as a control), and measured the accumulation of NO. Myr-Akt stimulates the basal production of NO from BLMVEC, whereas cells infected with β-galactosidase or activation-deficient Akt released small amounts of NO that were close to the limits of detection (Fig. 4a). These results, in conjunction with the results in COS cells, indicate that phosphorylation of eNOS by Akt is sufficient to regulate NO production at resting levels of calcium. Indeed, NOS activity measured in lysates from myr-Akt-infected BLMVEC demonstrates that the sensitivity of the enzyme to activation by calcium, assayed at a fixed calmodulin concentration, is enhanced relative to NOS activity seen in BLMVEC infected with the β-galactosidase virus (Fig. 4b). The calcium sensitivity of NOS activity in cells infected with activation-deficient Akt was greatly suppressed relative to both myr-Akt and β-galactosidase-infected cells.

As mentioned above, treatment of endothelial cells with VEGF activates Akt[23] and the release of NO through a mechanism partially blocked by inhibitors of PI(3)K[15]. Indeed, treatment of quiescent endothelial cells with VEGF induces Akt and eNOS phosphorylation (approximately twofold) concomitant with NO release (see Supplementary Information). To examine the functional link between VEGF as an agonist for NO release and Akt activation, BLMVEC were infected with adenoviruses for myr-Akt, AA-Akt or β-galactosidase, and VEGF-stimulated NO release was quantified. Infection of endothelial cells with myr-Akt enhances VEGF-driven NO production, whereas AA-Akt attenuates NO release (Fig. 4c). These results indicate that Akt may participate in the signal transduction events required for both basal and stimulated NO production in endothelial cells.

Our data show that Akt can phosphorylate eNOS on Ser 1179 and that phosphorylation enhances the ability of the enzyme to generate NO. Our results indicate that stimuli that promote NO release through a PI(3)K-dependent mechanism, independent of elevations in intracellular calcium (insulin and shear stress[14,24,25]), will stimulate Akt, thus permitting the phosphorylation and activation of eNOS at resting levels of calcium (Figs 1, 4). This can occur contemporaneously with the recruitment of the NOS regulatory protein Hsp90[26], perhaps by stabilizing calmodulin previously bound to eNOS, thus resulting in NO release. In the case of G-protein-coupled receptors or receptor tyrosine kinases that mobilize intracellular calcium, we propose that agonist-dependent stimulation of PI(3)K[11] and/or activation of calmodulin-dependent protein kinase kinase (CaMKK)[27] will activate Akt to phosphorylate eNOS concomitantly with the increase in cytoplasmic calcium. The calcium-dependent activation of calmodulin will stimulate CaMKK and the recruitment of calmodulin and perhaps Hsp90 to eNOS, facilitating rapid eNOS activation and the burst-like release of NO. How phosphorylation of eNOS by Akt enhances NO release is not known, but it is likely to be related to changes in the sensitivity of the enzyme to calcium-activated calmodulin. This may occur by the introduction of a negative charge, either by phosphate or aspartate, thereby 'opening up' the structure (perhaps by removing the auto-inhibitory loop of eNOS[28]) and thus permitting activated calmodulin binding at lower calcium concentrations. Thus, regulation of NO production by Akt-dependent phosphorylation of eNOS may provide a novel therapeutic target for the design of drugs aimed at improving endothelial function in cardiovascular diseases associated with dysfunction in the synthesis or biological activity of NO, such as hypertension, atherosclerosis, heart failure and diabetes.

Note added in proof: While in review, a recent paper has demonstrated that AMP-activated kinase can phosphorylate human eNOS on Ser 1177, *in vitro* (Chen *et al. FEBS Lett.*, **443,** 285–289 (1999)). □

Methods

Cell transfections. The bovine eNOS, human iNOS and rat nNOS cDNAs in pcDNA3 and HA-tagged wild-type Akt, Akt (K179M) and myr-Akt in pCMV6 were generated by standard cloning methods. The myr-nNOS in pcDNA3 was generated by PCR, incorporating a new amino terminus containing the eNOS N-myristoylation consensus site (MGNLKSVG) fused in frame to the second amino acid of the nNOS coding sequence. In preliminary experiments in COS cells, this construct was N-myristoylated based on incorporation of ^{3}H-myristic acid (unlike native nNOS) and resulted in approximately 60% of the total protein being targeted into the membrane fraction of cells (only 5–10% of nNOS was membrane associated in COS cells). The putative Akt phosphorylation sites in eNOS were mutated using the Quick Change site-directed mutagenesis kit (Stratagene) according to the manufacturers instructions. All mutants were verified by DNA sequencing. We plated COS-7 cells (100 mm dish) and transfected them with the NOS (7.5–30 μg) and Akt (1 μg) plasmids using calcium phosphate. To balance all transfections, the expression vector for β-galactosidase cDNA was used. 24–48 h after transfection, the expression of appropriate proteins (40–80 μg) were confirmed by western blot analysis using eNOS mAb (9D10, Zymed), HA mAb (12CA5, Boehringer Mannheim), iNOS pAb (Zymed Laboratories) or nNOS mAb (Zymed Laboratories).

NO release from transfected COS cells. 24–48 h after transfection, media were processed for the measurement of nitrite (NO_2^-), the stable breakdown product of NO in aqueous solution, by NO-specific chemiluminescence as described[20]. Media were deproteinized and samples containing NO_2^- were refluxed in glacial acetic acid containing sodium iodide. Under these conditions, NO_2^- was quantitatively reduced to NO which was quantified by a chemiluminescence detector after reaction with ozone in a NO analyser (Sievers). In all experiments, NO_2^- release was inhibitable by a NOS inhibitor. In addition, NO_2^- release from cells transfected with the β-galactosidase cDNA was subtracted to control for background levels of NO_2^- found in serum or media. In some experiments, we used cGMP accumulation in COS cells as a bioassay for the production of NO as described.

NOS activity assays. We used the conversion of ^{3}H-L-arginine to ^{3}H-L-citrulline to determine NOS activity in COS cell or endothelial cell lysates as described[26].

Phosphorylation studies *in vivo* and *In vitro*. For *in vivo* phosphorylation studies, COS cells were transfected with the cDNAs for wild-type or S635/

© 1999 Macmillan Magazines Ltd

1179A eNOS and HA–Akt overnight. 36 h after transfection, we placed cells into dialysed serum-replete, phosphate-free Dulbecco's minimum essential medium supplemented with 80 μCi per ml of ^{32}P orthophosphoric acid for 3 h. Some cells were pretreated with wortmannin (500 nM) in the phosphate-free medium for 1 h and during the labelling. The lysates were collected and the eNOS was solubilized and partially purified by ADP Sepharose-affinity chromatography as previously described. ^{32}P incorporation into eNOS was visualized after SDS–PAGE (7.5%) by autoradiography, and the amount of eNOS protein was verified by western blotting for eNOS. For *in vitro* phosphorylation studies, we incubated recombinant eNOS purified from *Escherichia Coli* with wild-type or kinase-inactive Akt immunoprecipitated from transfected COS cells. eNOS was incubated with ^{32}P γ-ATP (2 μl, specific activity 3000Ci per mmol), ATP (50 μM) and DTT (1 mM), in a buffer containing HEPES (20 mM, pH = 7.4), $MnCl_2$ (10 mM), $MgCl_2$ (10 mM) and immunoprecipitated Akt for 20 min at room temperature. In experiments examining the *in vitro* phosphorylation of wild-type and mutant eNOS we incubated recombinant Akt (1 μg) purified from baculovirus-infected SF9 cells with wild-type or S1179A eNOS (2.4 μg, purified from *E. coli*) using essentially the same conditions as above. Proteins were resolved by SDS–PAGE and ^{32}P incorporation and the amount of protein was determined by Coomassie staining as above. In studies identifying the labelled eNOS peptide, we incubated immunoprecipitated Akt with recombinant eNOS as above. The sample was run on SDS–PAGE and the eNOS band digested in gel, and the resultant tryptic fragments were purified by RP-HPLC. Peptide mass and ^{32}P incorporation were monitored and the prominent labelled peak was further analysed by mass spectrometry. In other experiments, peptides corresponding to the potential Akt phosphorylation site were synthesized, purified by HPLC and verified by mass spectrometry (W. M. Keck Biotechnology Resource Center, Yale University School of Medicine). The wild-type peptide was ^{1174}RIRTQSFSLQERHLRGAVPWA^{1194} and the mutant peptide was identical except that Ser 1179 was changed to alanine. *In vitro* kinase reactions were done essentially as described above by incubating peptides (25 μg) with recombinant Akt (1 μg). Reactions were then spotted onto phosphocellulose filters and the amount of phosphate incorporated was measured by Cerenkov counting.

Adenoviral infections and NO release in endothelial cells. We cultured BLMVEC in either 100 mm dishes (for basal NO release and NOS activity assays) or C6 well plates (for stimulated NO) as described[18]. BLMVEC were infected with 200 MOI of adenovirus containing the β-galactosidase[29], HA-tagged, inactive phosphorylation mutant Akt (AA-Akt[30]) or carboxy-terminal HA-tagged constitutively active Akt (myr-Akt) for 4 h. The virus was removed and cells left to recover for 18 h in complete medium. In preliminary experiments with the β-galactosidase virus, these conditions were optimal for infecting 100% of the cultures. For measurement of basal NO production, medium was collected 24 h after the initial infection with virus. For measurement of stimulated NO release, cells were then washed with serum-free medium followed by stimulation with VEGF (40 ng ml^{-1}) for 30 min. In some experiments, we determined the calcium dependency of NOS 24 h after adenoviral infection. Infected cells were lysed in NOS assay buffer containing 1% NP40, and detergent soluble material was used for activity assays. Lysates were incubated with EGTA-buffered calcium to yield appropriate amounts of free calcium in the incubation.

Statistics. Data are expressed as mean ± s.e.m. Comparisons were made using a two-tailed Student's *t*-test or ANOVA with a post-hoc test where appropriate. Differences were considered to be significant at $P < 0.05$.

Received 23 February; accepted 19 April 1999.

1. Shesely, E. G. *et al.* Elevated blood pressures in mice lacking endothelial nitric oxide synthase. *Proc. Natl Acad. Sci. USA* **93,** 13176–13181 (1996).
2. Huang, P. L. *et al.* Hypertension in mice lacking the gene for endothelial nitric oxide synthase. *Nature* **377,** 239–242 (1995).
3. Rudic, R. D. *et al.* Direct evidence for the importance of endothelium-derived nitric oxide in vascular remodeling. *J. Clin. Invest.* **101,** 731–736 (1998).
4. Murohara, T. *et al.* Nitric oxide synthase modulates angiogenesis in response to tissue ischemia. *J. Clin. Invest.* **101,** 2567–2578 (1998).
5. Michel, T., Li, G. K. & Busconi, L. Phosphorylation and subcellular translocation of endothelial nitric oxide synthase. *Proc. Natl Acad. Sci. USA* **90,** 6252–6256 (1993).
6. Garcia-Cardena, G., Fan, R., Stern, D. F., Liu, J. & Sessa, W. C. Endothelial nitric oxide synthase is regulated by tyrosine phosphorylation and interacts with caveolin-1. *J. Biol. Chem.* **271,** 27237–27240 (1996).
7. Corson, M. A. *et al.* Phosphorylation of endothelial nitric oxide synthase in response to fluid shear stress. *Circ. Res.* **79,** 984–991 (1996).
8. Coffer, P. J., Jin, J. & Woodgett, J. R. Protein kinase B (c-Akt): a multifunctional mediator of phosphatidylinositol 3-kinase activation. *Biochem. J.* **335,** 1–13 (1998).
9. Franke, T. F., Kaplan, D. R. & Cantley, L. C. PI3K: downstream AKTion blocks apoptosis. *Cell* **88,** 435–437 (1997).
10. Downward, J. Mechanisms and consequences of activation of protein kinase B/Akt. *Curr. Opin. Cell Biol.* **10,** 262–267 (1998).
11. Murga, C., Laguinge, L., Wetzker, R., Cuadrado, A. & Gutkind, J. S. Activation of Akt/protein kinase B by G protein-coupled receptors. A role for alpha and beta gamma subunits of heterotrimeric G proteins acting through phosphatidylinositol-3-OH kinase gamma. *J. Biol. Chem.* **273,** 19080–19085 (1998).
12. Dimmeler, S., Assmus, B., Hermann, C., Haendeler, J. & Zeiher, A. M. Fluid shear stress stimulates phosphorylation of Akt in human endothelial cells: involvement in suppression of apoptosis. *Circ. Res.* **83,** 334–341 (1998).
13. Cardone, M. H. *et al.* Regulation of cell death protease caspase-9 by phosphorylation. *Science* **282,** 1318–1321 (1998).
14. Zeng, G. & Quon, M. J. Insulin-stimulated production of nitric oxide is inhibited by wortmannin. Direct measurement in vascular endothelial cells. *J. Clin. Invest.* **98,** 894–898 (1996).
15. Papapetropoulos, A., Garcia-Cardena, G., Madri, J. A. & Sessa, W. C. Nitric oxide production contributes to the angiogenic properties of vascular endothelial growth factor in human endothelial cells. *J. Clin. Invest.* **100,** 3131–3139 (1997).
16. Parenti, A. *et al.* Nitric oxide is an upstream signal of vascular endothelial growth factor-induced extracellular signal-regulated kinase1/2 activation in postcapillary endothelium. *J. Biol. Chem.* **273,** 4220–4226 (1998).
17. Liu, J., Hughes, T. E. & Sessa, W. C. The first 35 amino acids and fatty acylation sites determine the molecular targeting of endothelial nitric oxide synthase into the golgi region of cells: A green fluorescent protein study. *J. Cell Biol.* **137,** 1525–1535 (1997).
18. García-Cardeña, G., Oh, P., Liu, J., Schnitzer, J. E. & Sessa, W. C. Targeting of nitric oxide synthase to endothelial cell caveolae via palmitoylation: Implications for nitric oxide signaling. *Proc. Natl Acad. Sci. USA* **93,** 6448–6453 (1996).
19. Shaul, P. W. *et al.* Acylation targets emdothelial nitric-oxide synthase to plasmalemmal caveolae. *J. Biol. Chem.* **271,** 6518–6522 (1996).
20. Sessa, W. C. *et al.* The Golgi association of endothelial nitric oxide synthase is necessary for the efficient synthesis of nitric oxide. *J. Biol. Chem.* **270,** 17641–17644 (1995).
21. Liu, J., Garcia-Cardena, G. & Sessa, W. C. Palmitoylation of endothelial nitric oxide synthase is necessary for optimal stimulated release of nitric oxide: implications for caveolae localization. *Biochemistry* **35,** 13277–13281 (1996).
22. Kantor, D. B. *et al.* A role for endothelial NO synthase in LTP revealed by adenovirus- mediated inhibition and rescue. *Science* **274,** 1744–1748 (1996).
23. Gerber, H. P. *et al.* Vascular endothelial growth factor regulates endothelial cell survival through the phosphatidylinositol 3′-Kinase/Akt signal transduction pathway. Requirement for flk-1/kdr activation. *J. Biol. Chem.* **273,** 30336–30343 (1998).
24. Kuchan, M. J. & Frangos, J. A. Role of calcium and calmodulin in flow-induced nitric oxide production in endothelial cells. *Am. J. Physiol.* **266,** C628–636 (1994).
25. Ayajiki, K., Kindermann, M., Hecker, M., Fleming, I. & Busse, R. Intracellular pH and tyrosine phosphorylation but not calcium determine shear stress-induced nitric oxide production in native endothelial cells. *Circ. Res.* **78,** 750–758 (1996).
26. Garcia-Cardena, G. *et al.* Dynamic activation of endothelial nitric oxide synthase by Hsp90. *Nature* **392,** 821–824 (1998).
27. Yano, S., Tokumitsu, H. & Soderling, T. R. Calcium promotes cell survival through CaM-K kinase activation of the protein kinase-B pathway. *Nature* **396,** 584–587 (1998).
28. Salerno, J. C. *et al.* An autoinhibitory control element defines calcium-regulated isoforms of nitric oxide synthase. *J. Biol. Chem.* **272,** 29769–29777 (1997).
29. Smith, R. C. *et al.* p21CIP1-mediated inhibition of cell proliferation by overexpression of the gax homeodomain gene. *Genes Dev.* **11,** 1674–1689 (1997).
30. Alessi, D. R. *et al.* Mechanism of activation of protein kinase B by insulin and IGF-1. *EMBO J.* **15,** 6541–6551 (1996).

Supplementary information is available on *Nature*'s World-Wide Web site (http://www.nature.com) or as paper copy from the London editorial office of *Nature*.

Acknowledgements. We thank P. Martasek and B. S. Masters for recombinant eNOS; J. Liu for constructing and characterizing the myr-nNOS construct; D. Bredt and T. Billiar for NOS cDNAs; T. Zioncheck for human VEGF; Y. Chen for generating the eNOS S1179A *E. Coli* expression construct; and K. Williams, M. LoPresti and K. Stone in the Keck Facility for their help with identification of the eNOS phosphopeptides. This work was supported by grants from the NIH and American Heart Association. W.C.S. is an Established Investigator of the American Heart Association. J.P.G. is supported by fellowships from the Heart and Stroke Foundation of Canada and from FCAR.

Correspondence and requests for materials should be addressed to W.C.S. (e-mail: william.sessa@yale.edu).

Activation of nitric oxide synthase in endothelial cells by Akt-dependent phosphorylation

Stefanie Dimmeler*, Ingrid Fleming†, Beate Fisslthaler†, Corinna Hermann*, Rudi Busse† & Andreas M. Zeiher*

** Molecular Cardiology, Department of Internal Medicine IV, and † Institute of Cardiovascular Physiology, University of Frankfurt, Theodor-Stern-Kai 7, 60590 Frankfurt, Germany*

Nitric oxide (NO) produced by the endothelial NO synthase (eNOS) is a fundamental determinant of cardiovascular homeostasis: it regulates systemic blood pressure, vascular remodelling and angiogenesis[1–3]. Physiologically, the most important stimulus for the continuous formation of NO is the viscous drag (shear

© 1999 Macmillan Magazines Ltd